

Available online at www.sciencedirect.com

ScienceDirect

Procedia Technology 00 (2014) 000–000

Procedia
Technology

www.elsevier.com/locate/procedia

CENTERIS 2014 - Conference on ENTERprise Information Systems / ProjMAN 2014 -
International Conference on Project MANagement / HCIST 2014 - International Conference on
Health and Social Care Information Systems and Technologies

Systematic exploitation of the persistent scatterer interferometry potential

Michele Crosetto^{a,*}, Núria Devanthery^a, María Cuevas-González^a,
Oriol Monserrat^a, Donato Petracca^a, Bruno Crippa^b

^aCentre Tecnològic de les Telecomunicacions de Catalunya (CTTC), Geomatics Division, Av. Gauss 7, E-08860, Castelldefels (Barcelona), Spain

^bDepartment of Earth Sciences, University of Milan, Via Cicognara 7, I-20129, Milan, Italy

Abstract

This paper briefly addresses the problem of exploiting the potential of Persistent Scatterer Interferometry (PSI) data. This has always been an open issue with the previous SAR missions. With Sentinel-1 it is becoming even more important due to its high throughput. Current data processing capabilities allow us to process a fraction of the acquired data; and the data analysis and exploitation only cover a part of the PSI results. From one side the PSI processing tools require to be improved, while from the other side there is the need of increasing the capabilities to analyze and interpret the PSI results, thus exploiting their potential.

© 2014 The Authors. Published by Elsevier Ltd.

Peer-review under responsibility of the Organizing Committees of CENTERIS/ProjMAN/HCIST 2014

Keywords: SAR: radar: deformation monitoring.

1. Introduction

This paper is focused on the exploitation of the potential of Persistent Scatterer Interferometry (PSI) for deformation monitoring. Differential Interferometric Synthetic Aperture Radar (DInSAR) and PSI techniques have experienced a

* Corresponding author. Tel.: +34-93-556-9294; fax: +34-93-556-9292.

E-mail address: mcrosetto@cttc.cat

major development in the last two decades. Most of the development has been done using C-band data from ERS-1/2, Envisat and Radarsat. The data acquired by these satellite cover long periods of time, a key aspect to guarantee a long-term deformation monitoring. PSI has experienced a major step forward since 2007 with the advent of very high resolution X-band data, e.g. see [1]. This includes the capability to generate a dense sampling of Persistent Scatterers (PSs), a high sensitivity to small displacements and a remarkable quality improvement of the time series with respect to the C-band. A significant improvement is expected with the data coming from the C-band sensor onboard the Sentinel-1 satellite, launched on 3 April 2014. Sentinel-1 will improve the data acquisition throughput with respect to previous sensors, increasing considerably the PSI deformation monitoring potential.

With the advent of Sentinel-1 the aspect of exploitation of the above PSI potential will become very important, which, on the other hand, has always been an open issue with any SAR sensor. The problem can be summarized in this way: the PSI data processing capabilities allow us to process a fraction of the data acquired by the SAR satellites; and the data analysis, interpretation and exploitation only covers a part of the PSI-generated results. The problem is therefore two-fold: from one side there is the need of improving the PSI processing tools, to achieve massive and systematic data processing capabilities; from the other side there is the need of increasing the capabilities to correctly analyze and properly interpret the PSI results, thus exploiting their potential.

This paper addresses the above two aspects by considering the experience of the authors to process and analyze the PSI results obtained from a full frame of very high resolution TerraSAR-X data, which cover more than 1000 km² over the metropolitan area of Barcelona.

2. PSI processing

This section concerns the tools needed to process a vast amount of PSI data. It concisely describes the key features of the PSI chain of the Geomatics (PSIG) Division of CTTC, which has been successfully tested processing a full frame of very high resolution X-band PSI data. A complete description of the procedure is given in [2].

The inputs of PSIG include a stack of N co-registered SAR images and M wrapped interferograms, with $M \gg N$: typically more than 10 interferograms per image are used. The procedure includes three main processing blocks. The goal of the first block is obtaining a set of correctly unwrapped and temporally ordered phases, which are computed over PSs that cover the area of interest homogeneously. In the second block, the abovementioned phases are used to estimate the Atmospheric Phase Screen (APS) using spatio-temporal filters. Finally, the deformation time series are computed on a dense set of PSs in the third block. The main processing steps are described below.

- Candidate Cousin PS (CPS) selection: a set of PSs with phases characterized by a moderate spatial variation is sought. This is accomplished by using at least a seed PS and searching for its “cousins”, i.e. PSs with similar characteristics. An iterative process is used to ensure an appropriate CPS coverage and density.
- 2D phase unwrapping, which is performed on the candidate CPSs using the redundant set of M interferograms. An implementation of the Minimum Cost Flow method [3,4] is used in this step.
- Phase unwrapping consistency check. This check is based on a LS estimation, followed by the analysis of the so-called residuals. The final set of CPSs is selected at this stage.
- APS estimation and removal. Using the selected CPSs, the APS is estimated using spatio-temporal filters [5,6]. The APS is then removed from the original interferograms, obtaining a set of M APS-free interferograms.
- The deformation velocity and Residual Topographic Error (RTE) are computed over a dense set of PSs (denser than the selected CPSs), from the M wrapped APS-free interferograms, using the method of the periodogram. Optionally, an extension of the two-parameter model can be used to account for the thermal expansion [7].
- The RTE phase component is removed from the wrapped APS-free interferograms. The linear deformation component can optionally be removed and then, in a later stage, added back to the deformation time series. The same procedure can be done with the thermal expansion component.
- A 2+1D phase unwrapping is executed on the set of M APS- and RTE-free interferograms to obtain the final deformation phase time series and a quality index for each time series.

As said, the PSIG chain has been tested using different X-band PSI datasets. The authors are working on its extension to allow the processing of Sentinel-1 data. Most efforts are focused on reducing the processing time and, more importantly, to reduce all processing steps that require the human intervention, e.g. input data preparation and quality check of the main processing steps.

3. PSI data interpretation

This section briefly addresses the aspects of PSI data analysis, interpretation and exploitation. This aspect, which is fundamental to fully exploit the PSI deformation monitoring capabilities, is the one that requires more human involvement. We can distinguish two major steps. The first one involves a preliminary analysis and interpretation of the PSI results. This is a fundamental task of screening the PSI results, which may concern hundreds of different types of deformation phenomena. The second steps concerns the exploitation of the PSI results, which ideally involves the identification of an end user and which may require the analysis of PSI data and many other additional data by an expert of the specific phenomenon at hand.

The screening of the PSI results is a fundamental task, considering that a single frame can contain hundreds of different deformation phenomena. The screening usually requires basic cartographic information, including the topography of the covered area: tools like Google Earth offer a valuable support to the screening. An appropriate screening needs appropriate procedures to consider the specific characteristics of PSI data, e.g.:

- PS spatial sampling has an opportunistic character. While in some areas, like cities, PSI obtains a reasonably good sampling, in others, like vegetated and forested areas, PSI tends to systematically fail.
- Due to the ambiguous nature of PSI observations, PSI suffers limitations in its capability to measure “fast” deformation phenomena. This limitation basically depends on the spatial pattern of the deformation, its PS sampling density and the temporal SAR sampling.
- Many PSI approaches resolve the unwrapping phase by assuming a linear deformation model for deformation. This can have a negative impact on the PSI estimates for all deformation phenomena characterized by non-linear temporal deformation, i.e. where this assumption is not valid. In areas where the deformation shows “significantly non-linear motion” the PSI products may lack PSs, because the observations do not fit the assumed linear model.
- Deformation tilts or trends. PSI deformation rates may sometimes contain spatial tilts or trends, which can be due either to uncompensated orbital errors or low frequency residual atmospheric effects.
- The deformation measurements estimated with the PSI technique refer to the Line-of-sight (LOS) of the used SAR sensor. Given a generic 3D deformation, PSI provides the estimate of the LOS component of this deformation (i.e. the projection of the 3D deformation in the LOS direction). This aspect is particularly important when analyzing landslides: their correct interpretation needs to consider the local topography.

4. TerraSAR-X PSI results over the metropolitan area of Barcelona

This section describes the results obtained using 42 TerraSAR-X images and 633 interferograms that cover the period from December 2007 to June 2012. The deformation velocity map of the full frame image is shown in Fig. 1. It comprises more than 5.4 million PSs and covers 1019 km². The following figures illustrate some examples of results of the screening of the PSI results.

- The first example, shown in Fig. 2, concerns a subsidence of a road embankment. In this case the ground motion seems to be a consequence of soil compaction of the recently constructed road. The LOS displacement rates in the observed period reach 10 mm/yr.
- The second example, shown in Fig. 3, illustrates two subsidence phenomena. The first one concerns several recently constructed access roads, while the second one affects a portion of the high-speed railway embankment. In the latter case the LOS displacement rates reach a maximum of about 9 mm/yr.
- The third example, shown in Fig. 4, illustrates what appears to be an uplift that affects a portion of a highway embankment. A preliminary interpretation, based on the geomorphology of the area, suggests that this area is affected by a landslide.
- The fourth example, shown in Fig. 5, illustrates the surface effects associated with the construction works of a new underground station.
- The last example, shown in Fig. 6, concerns an uplift that is probably related to the stop of water extraction activities in an industrial area. The LOS displacement rates reach a maximum of about 4 mm/yr over the 2007-2012 observed period.

Acknowledgements

This work has been partially founded by the Fundaci3n Ciudad de la Energ3a (<http://www.ciuden.es>). Six of the 28 TerraSAR-X SAR images used in the Barcelona case study were acquired within the Project “Evaluation of DEM derived from TerraSAR-X data, LAN0634”, of the TerraSAR-X Science Service Program.

References

- [1] Crosetto, M., Monserrat, O., Iglesias, R., Crippa, B. “Persistent scatterer interferometry: Potential, limits and initial C- and X-band comparison”, *Photogrammetric Engineering and Remote Sensing*, vol. 76, no. 9, pp. 1061–1069, September 2010.
- [2] Devanthery, N., Crosetto, M., Monserrat, O., Cuevas-Gonzalez, M., Crippa, B. An approach to Persistent Scatterer Interferometry: the PSIG chain. Submitted to *Remote Sensing*.
- [3] Costantini, M. (1998). A novel phase unwrapping method based on network programming. *IEEE TGRS*, 36, 3, 813–821.
- [4] Costantini, M., Farina, A., & Zirilli, F. (1999). A fast phase unwrapping algorithm for SAR interferometry. *IEEE TGRS*, 37, 1, 452–460.
- [5] Ferretti, A., Prati, C. & Rocca, F. (2000). Nonlinear subsidence rate estimation using permanent scatterers in differential SAR interferometry. *IEEE Transactions on Geoscience and Remote Sensing*, 38, 5, 2202–2212.
- [6] Berardino, P., Fornaro, G., Lanari, R., & Sansosti, E. (2002). A new algorithm for surface deformation monitoring based on small baseline differential SAR interferograms. *IEEE TGRS*, 40, 11, 2375–2383.
- [7] Monserrat, O., Crosetto, M., Cuevas, M., & Crippa, B. (2011). The thermal expansion component of Persistent Scatterer Interferometry observations. *IEEE Geoscience and Remote Sensing Letters*, 8, 864–868.

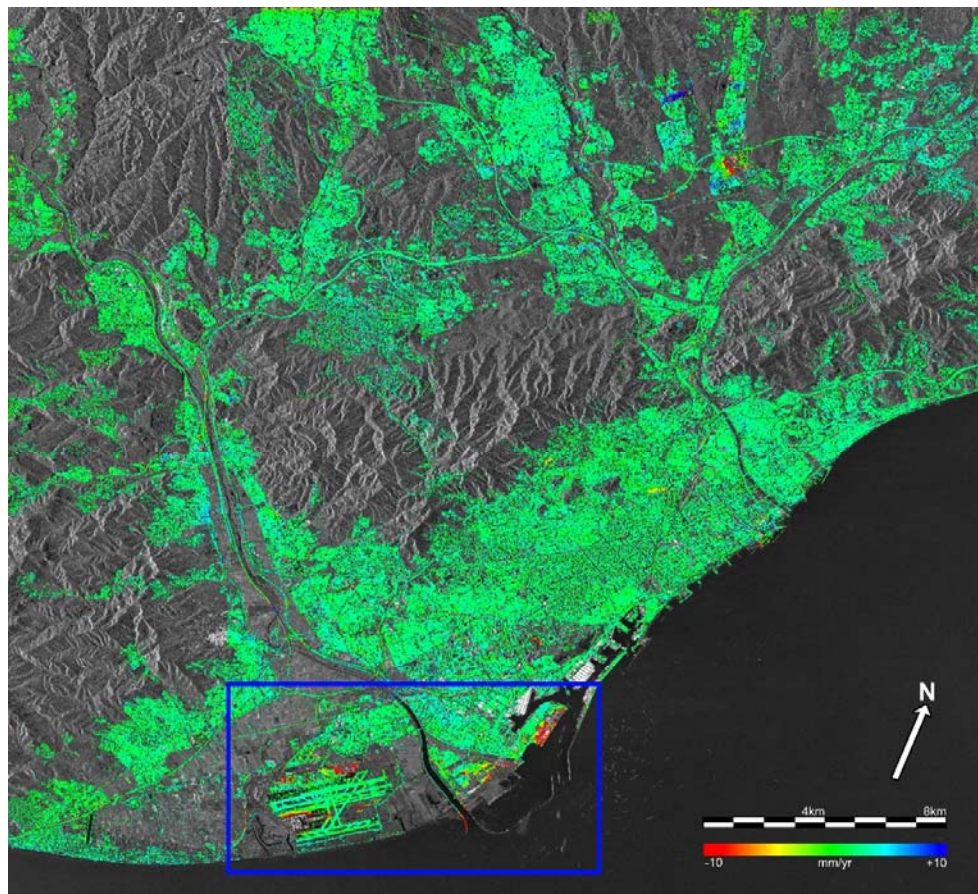


Fig. 1. Velocity map obtained from TerraSAR-X PSI over the metropolitan area of Barcelona superposed to a SAR amplitude image. The blue frame indicates the area of the airport and port of Barcelona

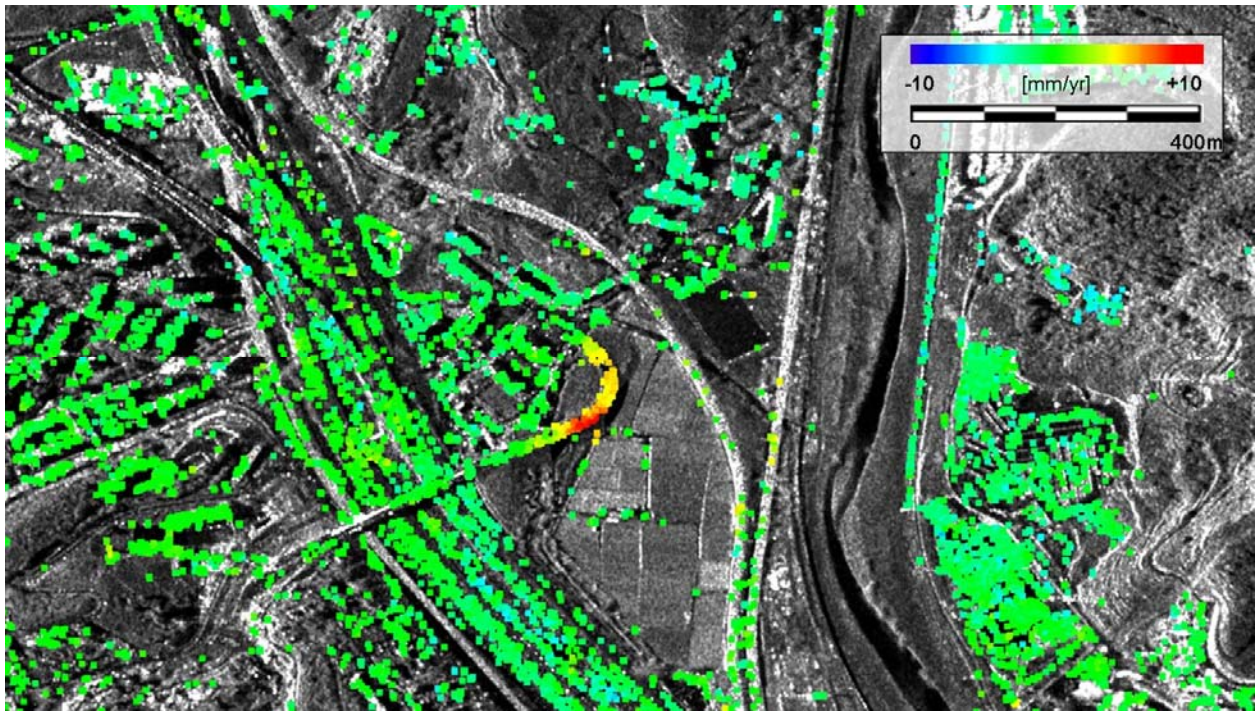


Fig. 2. Subsidence of a road embankment.

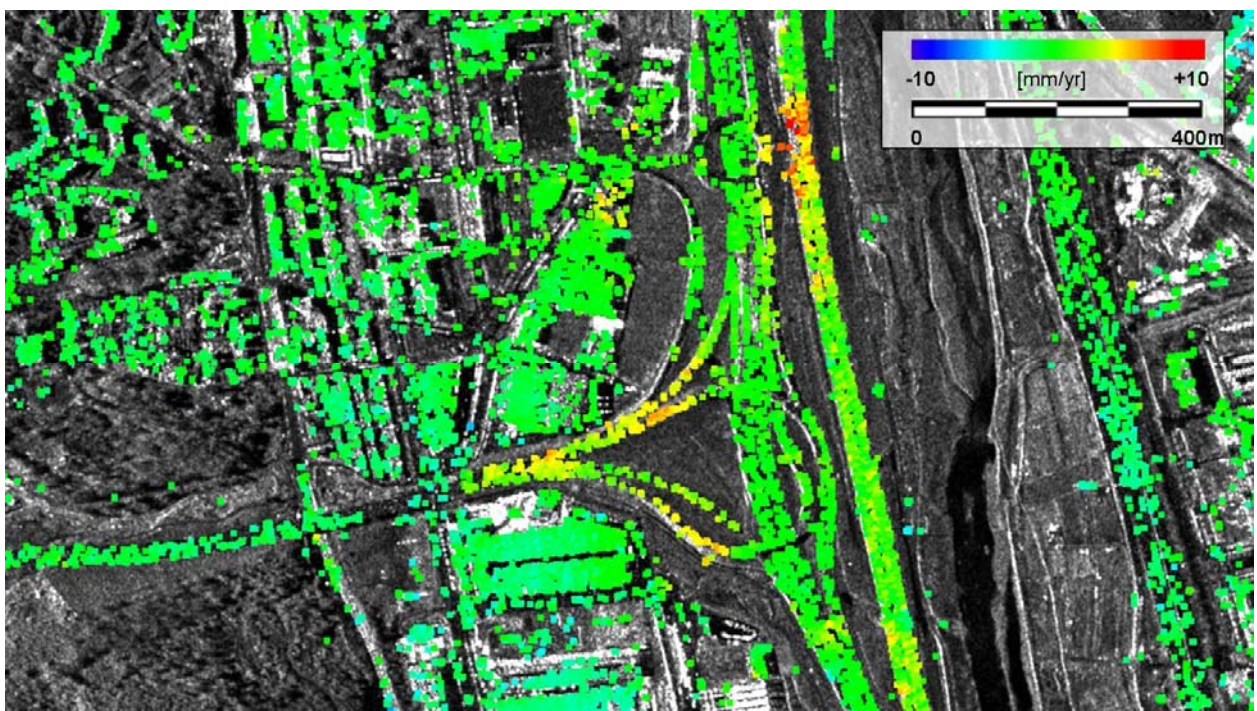


Fig. 3. Subsidence affecting access roads and a portion of the high-speed railway embankment.

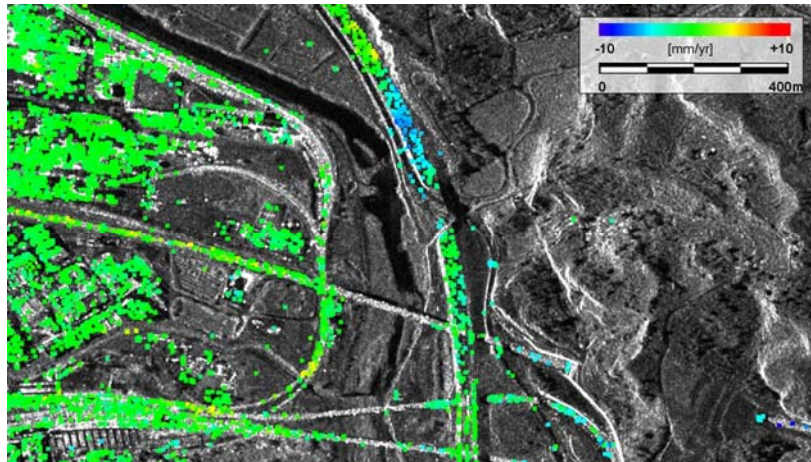


Fig. 4. Effect on a highway embankment, probably caused by a landslide.

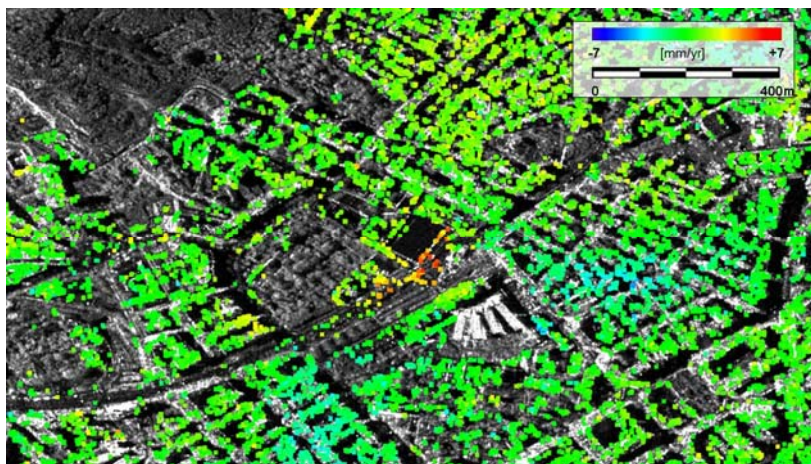


Fig. 5. Subsidence caused by the construction of an underground station.

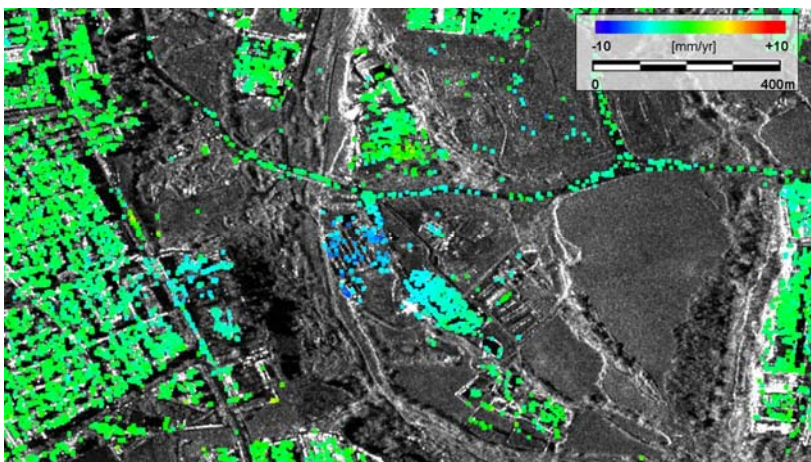


Fig. 6. Uplift probably related to the stop of water extraction activities.